Journal of Alloys and Compounds 499 (2010) 149–153

Contents lists available at ScienceDirect

Journal of Alloys and Compounds

journal homepage: www.elsevier.com/locate/jallcom

Effect of Cu concentration, solder volume, and temperature on the reaction between SnAgCu solders and Ni

S.C. Yang, C.C. Chang, M.H. Tsai, C.R. Kao*

Department of Materials Science and Engineering, National Taiwan University, Taipei City, Taiwan

ARTICLE INFO

Article history:
Received 21 December 2009
Received in revised form 18 March 2010
Accepted 18 March 2010
Available online 25 March 2010

Keywords:
Soldering
Intermetallics
Diffusion

ABSTRACT

The interfacial reaction between SnAgCu and Ni is influenced by three important factors, namely, the Cu concentration in solder, solder volume, and temperature. In our previous studies, the first two factors had been investigated individually. In this study, the effects of these three factors are studied concurrently. Three different sizes of solder spheres (300, 500, and 760 μm in diameter) with three different Cu concentrations (0.3, 0.5, and 0.7 wt.%) are used. The aging temperatures are 160 and 180 °C. It is found that as the residual apparent Cu concentration in the solder decreases and the solder volume reduces, the type of intermetallic compound changes from $(Cu,Ni)_6Sn_5$ to $(Ni,Cu)_3Sn_4$. This study confirms that the critical Cu concentration decreases as the temperature decreases. In addition, the massive spalling phenomenon, which tends to occur in a liquid–solid reaction, is not observed in the solid-solid reaction.
© 2010 Elsevier B.V. All rights reserved.

1. Introduction

In our previous studies, a strong Cu-concentration effect between SnAgCu and Ni was reported [1–4]. With a slight increase in Cu concentration, the reaction product changed from $(Ni,Cu)_3Sn_4$ to $(Cu,Ni)_6Sn_5$. At 235 °C, the critical Cu concentration for such a change was 0.4 wt.% [1–4]. In addition to our reports, several papers had also been published on this subject [5–7]. To understand the interfacial reactions and the reaction mechanisms, the equilibrium phase relationship is a powerful tool. The important ternary Sn–Cu–Ni system has been investigated by various groups [8–11]. Recently, Yu et al. [12], using thermodynamic calculation (the CALPHAD approach), predicted that the critical Cu concentration was in fact a strong function of temperature. It decreases with decreasing temperature [12]. In other words, temperature is also an important factor in the reaction between SnAgCu and Ni.

In addition to the Cu concentration and temperature, solder volume is also known to be an important factor in many soldering reactions [13–17], and several studies have reported the effect of solder volume on the reaction between SnAgCu and Ni [18–21]. This solder-volume effect on the reaction between SnAgCu and Ni can be attributed to the limited supply of Cu atoms. With the growth of Cu-bearing intermetallics, the available Cu in the solder decreases and the Cu concentration decreases accordingly. Excessive decrease in Cu concentration might change the equilibrium of the intermetallic at the interface. In short, the solder-volume effect is a particular type of expression of the Cu-concentration effect.

The objective of this study is two-fold. The first is to experimentally verify the temperature effect predicted by Yu et al. [12]. The second is to gain an understanding of the combined effect of Cu concentration, solder volume, and temperature on the reaction between SnAgCu and Ni.

2. Experimental procedure

Fig. 1 shows the schematic drawing of the solder joints used in this study. Solder balls with three different Cu concentrations (Sn3AgxCu, x = 0.3, 0.5, and 0.7 wt.%) and three different diameters (300, 500, and 760 μm) were used. The contact pads had only a Ni layer over Cu (*i.e.* without a gold layer over Ni). The pad opening diameter was 375 μm. The Ni layer was electrolytically plated and free of phosphorous.

Before reflow, all substrates were dipped into a dilute hydrochloric acid solution and then fluxed. Then, the solder balls were placed on the pads manually. Thereafter, samples were reflowed with a typical profile (235 °C peak temperature and 90 s molten solder duration). It was possible that solder balls of different sizes experienced slightly different thermal histories. But we believe that this effect is relatively weak. The smaller balls tended to melt earlier than larger balls, but they also solidified earlier than the larger ones. After reflow, the samples were subjected to aging at 160 or 180 °C for 1000 h.

The compositions of the reaction products were determined using a field-emission electron microanalyzer (FE-EPMA, JEOL JXA-850F). In microprobe analysis, the concentration of each element was measured independently, and the total weight percentage of all the elements was within 100 (±2) wt.% in each case. The mean thickness of the interfacial intermetallic layers for various times was measured with the aid of image-processing software. The thickness was defined as the total area occupied by the intermetallic divided by the linear length of the interface.

3. Results

According to the results obtained in this study, $(Cu,Ni)_6Sn_5$ and $(Ni,Cu)_3Sn_4$ are the only two compounds that are formed at the interface. In the following, the results are presented according to the initial Cu concentration in the solders. For the microstructures

* Corresponding author. Tel.: +886 2 3366 3745; fax: +886 2 3366 3745.
E-mail address: crkao@ntu.edu.tw (C.R. Kao).

0925-8388/$ – see front matter © 2010 Elsevier B.V. All rights reserved.
doi:10.1016/j.jallcom.2010.03.168

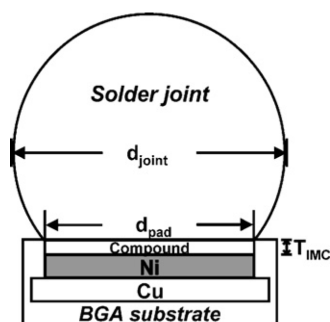

Fig. 1. Schematic diagram showing a Sn3AgxCu solder sphere soldered onto a Ni pad.

after aging, only the results obtained after aging at 160 °C are presented in detail. The micrographs of the solder joints aged at 180 °C are omitted for the sake of brevity. For aging at 180 °C, only the key data are summarized in Table 1.

3.1. Sn3Ag0.7Cu spheres

The interfaces for the Sn3Ag0.7Cu cases after reflow are shown in Fig. 2(a)–(c). Different solder volumes were used in each case. In each case, only a needle-like $(Cu,Ni)_6Sn_5$ layer formed at the interface. In Fig. 2 (and in all the other micrographs shown in Figs. 3 and 4), the composition marked on the upper-left corner of each micrograph is the initial solder sphere composition, and it does not reflect the actual Cu concentrations after reflow or aging. The Cu concentration after reflow or aging differed from the initial Cu concentration because some of the Cu atoms originally in the

Table 1
Apparent Cu concentration and intermetallic(s) formed at the interface for different experimental conditions.

Solder sphere diameter (μm)	Initial Cu conc. (wt.%)	After reflow (235 °C, 90 s)		After aging (180 °C, 1000 h)		After aging (160 °C, 1000 h)	
		Apparent Cu conc. (wt.%)	Type of intermetallic formed at interface	Apparent Cu conc. (wt.%)	Type of intermetallic formed at interface	Apparent Cu conc. (wt.%)	Type of intermetallic formed at interface
760	0.7	0.68	$(Cu,Ni)_6Sn_5$	0.57	$(Cu,Ni)_6Sn_5$	0.67	$(Cu,Ni)_6Sn_5$
	0.5	0.48	$(Cu,Ni)_6Sn_5$	0.36	$(Cu,Ni)_6Sn_5$	0.47	$(Cu,Ni)_6Sn_5$
	0.3	0.30	$(Ni,Cu)_3Sn_4$	–	–	0.28	$(Cu,Ni)_6Sn_5$
500	0.7	0.65	$(Cu,Ni)_6Sn_5$	0.27	$(Cu,Ni)_6Sn_5$	0.61	$(Cu,Ni)_6Sn_5$
	0.5	0.39	$(Cu,Ni)_6Sn_5$	–	–	0.37	$(Cu,Ni)_6Sn_5$
	0.3	0.30	$(Ni,Cu)_3Sn_4$	0.18	$(Ni,Cu)_3Sn_4$	0.18	$(Cu,Ni)_6Sn_5/(Ni,Cu)_3Sn_4$
300	0.7	0.40	$(Cu,Ni)_6Sn_5$	0.18	$(Ni,Cu)_3Sn_4$	0.2	$(Cu,Ni)_6Sn_5/(Ni,Cu)_3Sn_4$
	0.5	0.20	$(Ni,Cu)_3Sn_4$	0	$(Ni,Cu)_3Sn_4$	0.16	$(Ni,Cu)_3Sn_4$
	0.3	0.24	$(Ni,Cu)_3Sn_4$	0	$(Ni,Cu)_3Sn_4$	0	$(Ni,Cu)_3Sn_4$

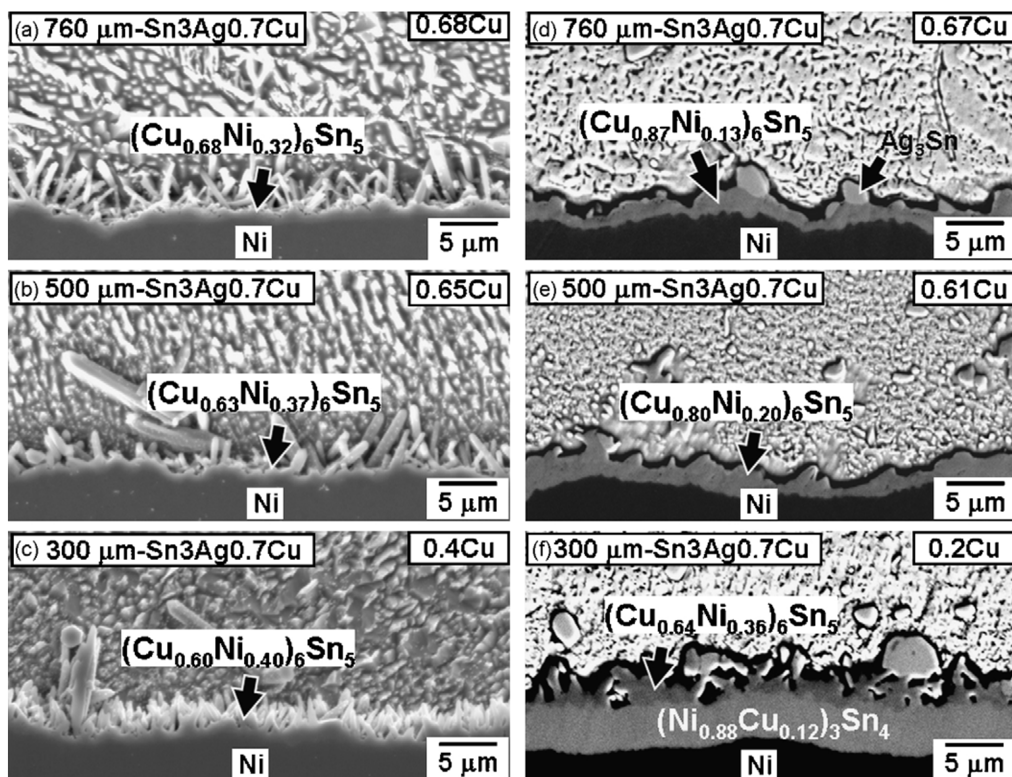

Fig. 2. Cross-section SEM images for Sn3Ag0.7Cu solder joints of different solder volumes after reflow at 235 °C for 90 s [(a)–(c)], and after subsequently aging at 160 °C for 1000 h [(d)–(f)]. The composition marked on the upper-left corner of each micrograph is the initial solder sphere composition, and the number on the upper-right corner is the apparent Cu concentration after reflow or aging.

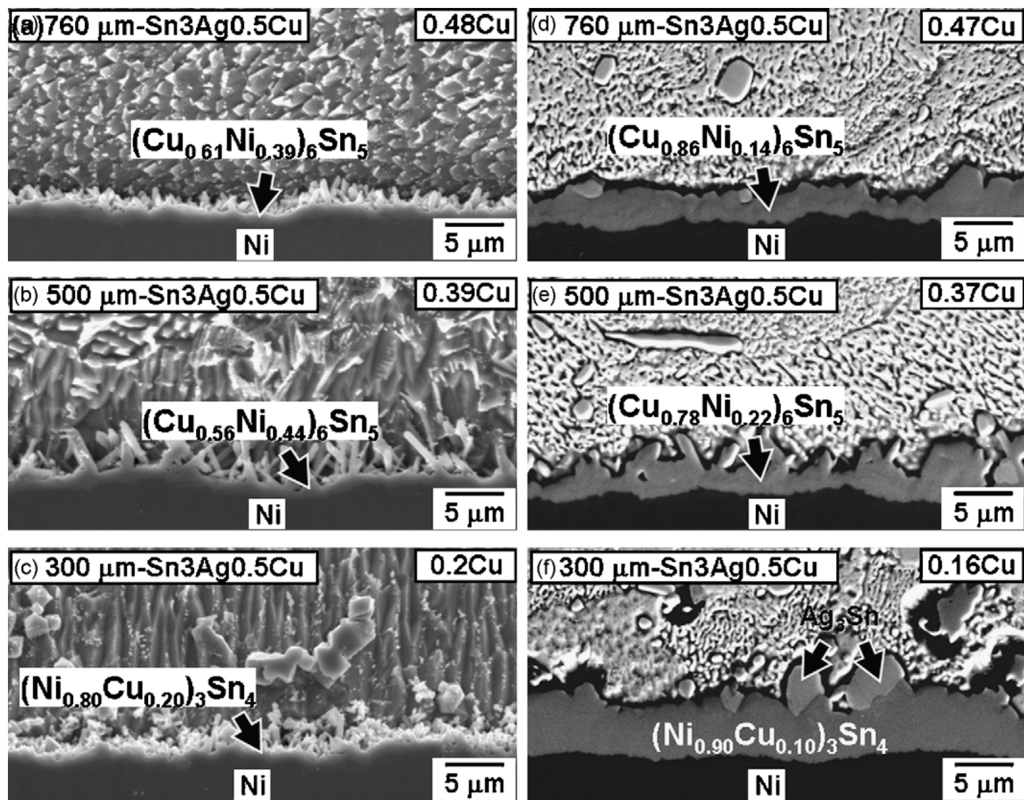

Fig. 3. Cross-section SEM images for Sn3Ag0.5Cu solder joints of different solder volumes after reflow at 235 °C for 90 s [(a)–(c)], and after subsequently aging at 160 °C for 1000 h [(d)–(f)]. The composition marked on the upper-left corner of each micrograph is the initial solder sphere composition, and the number on the upper-right corner is the apparent Cu concentration after reflow or aging.

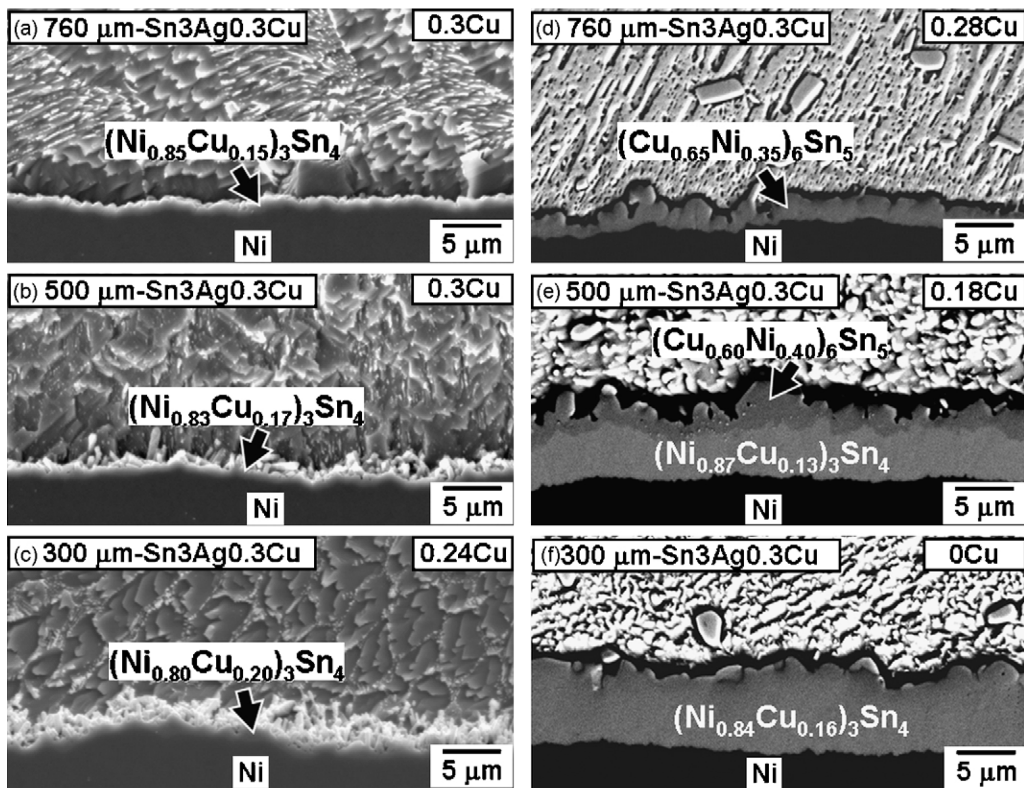

Fig. 4. Cross-section SEM images for Sn3Ag0.3Cu solder joints of different solder volumes after reflow at 235 °C for 90 s [(a)–(c)], and after subsequently aging at 160 °C for 1000 h [(d)–(f)]. The composition marked on the upper-left corner of each micrograph is the initial solder sphere composition, and the number on the upper-right corner is the apparent Cu concentration after reflow or aging.

solder were incorporated into the intermetallic(s) at the interface. The estimated Cu concentration inside the solder after reflow or aging ("the apparent Cu concentration") is marked (in wt.%) on the upper-right corner of each micrograph. The method for estimating the apparent Cu concentration will be presented later. The values of the apparent Cu concentration and the intermetallics formed at the interface for different conditions are summarized in Table 1. The apparent Cu concentrations for the 760, 500, and 300 μm cases after reflow are 0.68, 0.65, and 0.4 wt.%, respectively.

Fig. 2(d)–(f) shows the microstructures of the interfaces after aging at 160 °C for 1000 h. For the larger solder joints (760 and 500 μm), there was still only a $(Cu,Ni)_6Sn_5$ layer at the interface, as shown in Fig. 2(d) and (e). However, for the smallest solder joint (300 μm), a layer of $(Ni,Cu)_3Sn_4$ had nucleated and grew between the $(Cu,Ni)_6Sn_5$ and Ni, as shown in Fig. 2 (f). The values of the apparent Cu concentration for the 760, 500, and 300 μm cases after aging are 0.67, 0.61, and 0.2 wt.%, respectively.

3.2. Sn3Ag0.5Cu spheres

As shown in Fig. 3(a) and (b), for larger solder joints (760 and 500 μm) after reflow, the results for Sn3Ag0.5Cu were similar to those of Sn3Ag0.7Cu. Only $(Cu,Ni)_6Sn_5$ formed at the interface after reflow. However, for the smallest solder joint (300 μm), $(Ni,Cu)_3Sn_4$, instead of $(Cu,Ni)_6Sn_5$, formed at the interface after reflow, as shown in Fig. 3(c).

During subsequent aging at 160 °C for 1000 h, for larger solder joints (760 and 500 μm), the results for Sn3Ag0.5Cu were similar to those of Sn3Ag0.7Cu, as shown in Fig. 3(d) and (e). Only $(Cu,Ni)_6Sn_5$ formed at the interface. For the smallest solder joint (300 μm), only a layer of $(Ni,Cu)_3Sn_4$ formed at the interface, as shown in Fig. 3(f).

3.3. Sn3Ag0.3Cu spheres

As shown in Fig. 4(a)–(c), when the initial Cu concentration was 0.3 wt.%, the reaction product was $(Ni,Cu)_3Sn_4$ after reflow. This result is consistent with previous reports [2,3] that only $(Ni,Cu)_3Sn_4$ formed after reflow at the interface as Cu concentration was below 0.4 wt.%.

After solid-state aging, only $(Cu,Ni)_6Sn_5$ was observed in the 760-μm solder sphere, as shown in Fig. 4(d), and the original $(Ni,Cu)_3Sn_4$ that had formed after reflow had disappeared. A similar observation has been reported in the literature [22,23], namely, that the Ni_3Sn_4 layer could be converted to $(Cu,Ni)_6Sn_5$. The formation of $(Cu,Ni)_6Sn_5$ at such a low Cu concentration seems to be inconsistent with the results reported in the literature [2,3], but was in fact consistent with the prediction of Yu et al. [12]. An explanation for this will be presented in the Section 4.

In the 500-μm solder joint after aging, both $(Cu,Ni)_6Sn_5$ and $(Ni,Cu)_3Sn_4$ were formed at the interface, as shown in Fig. 4(e). As the joint shrunk to 300 μm, as shown in Fig. 4(f), there was only $(Ni,Cu)_3Sn_4$ at the interface after aging.

4. Discussion

The critical Cu concentration for Sn3.5AgCu as calculated by Yu et al. [12] is shown by the dashed curve in Fig. 5. The critical Cu concentration at each temperature represents the Cu concentration of the Sn-rich corner of the $(Sn)+(Cu_6Sn_5)+(Ni_3Sn_4)$ tie triangle for the SnCuNi isotherm at that particular temperature, *i.e.*, point O in Fig. 7 of Ref. [5]. As the compositions of the three vertices in a typical ternary isotherm are functions of temperature, the critical Cu concentration also depends on temperature. It is this temperature dependence that gives rise to the dashed curve in Fig. 5. According to the calculation of Yu et al. [12], the critical Cu concentration decreases with temperature. Also shown in Fig. 5 are data

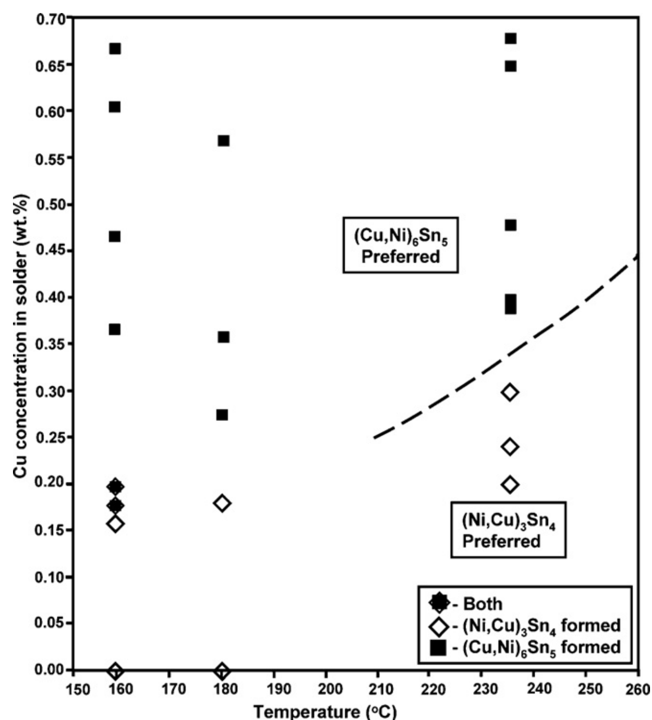

Fig. 5. The dash curve, calculated by Yu et al. [12], shows the critical Cu concentration for Sn3.5AgCu solders as a function of temperature. Solid squares and hollow diamonds are obtained from the present study, and denote the formation of $(Cu,Ni)_6Sn_5$ and $(Ni,Cu)_3Sn_4$, respectively.

points obtained from this study, showing the intermetallic compounds observed at the interface. These data points reveal that the dashed curve is correct not only in its qualitative trend but also in its quantitative accuracy. In plotting the data points in Fig. 5, the Cu concentrations used are the apparent Cu concentrations. The rationalization for using this apparent concentration and the method of estimating this concentration are presented in the following.

As pointed out in our previous studies [18,19], the Cu concentration in solder would decrease with the formation of Cu-bearing intermetallics, $(Cu,Ni)_6Sn_5$ and $(Ni,Cu)_3Sn_4$, at the interface. As the Cu concentration decreases and becomes smaller than the critical Cu concentration, the stable compound at the interface also changes. From the mass balance of Cu, the total amount of Cu inside the solder and inside the intermetallic(s) equals the initial amount of Cu in the solder. From this mass balance consideration, we obtain [18,19]

$$w_{Cu} - w_{Cu}^0\,[\text{wt.\%}] = -\left(\frac{d_{pad}^2}{d_{joint}^3}\right)(n_1 T_{(Cu,Ni)_6Sn_5} + n_2 T_{(Ni,Cu)_3Sn_4}) \quad (1)$$

where w_{Cu} and w_{Cu}^0 represent the apparent and initial Cu concentrations in the solder, respectively. The symbols d_{joint} and d_{pad} represent the diameters (in μm) of the solder ball and the opening on the pad on the substrate, respectively. The symbol T represents the thickness (in μm) of the intermetallic compound, with the subscript identifying the type of compound. The symbols n_1 and n_2 depend on the composition of $(Cu,Ni)_6Sn_5$ and $(Ni,Cu)_3Sn_4$. For example, the n_1 values for Cu_6Sn_5 and $(Cu_{0.6}Ni_{0.4})_6Sn_5$ are 64 and 40, respectively; n_2 values for Ni_3Sn_4 and $(Ni_{0.8}Cu_{0.2})_3Sn_4$ are 0 and 10, respectively. The apparent Cu concentrations according to Eq. (1) are listed in Table 1 and labeled on the micrographs shown in Figs. 2–4. The results in Table 1 are also used to plot the data points in Fig. 5.

According to the calculation of Yu et al. [12] (dashed curve, Fig. 5), the critical Cu concentration for a 240 °C reflow is 0.34 wt.%.

The results of this study confirm that the critical Cu concentration is between 0.39 and 0.3 at 240 °C (see third and fourth columns of Table 1). The results of this study at lower temperatures (160 and 180 °C) are also consistent with the extrapolation of the dashed curve in Fig. 5.

5. Conclusion

The prediction by Yu et al. [12]—that the critical Cu concentration is temperature dependent—has been experimentally verified in this study. The prediction that the critical Cu concentration decreases with decreasing temperature is correct not only in its qualitative trend but also in its quantitative accuracy.

This study also points out that the interfacial reaction between SnAgCu and Ni is influenced by three important factors, namely, the Cu concentration in solder, temperature, and the solder volume. The first factor expresses itself through the critical Cu concentration. The second factor is important in that the critical Cu concentration decreases with temperature. The third factor is important because it limits the availability of Cu atoms in the solder. As the solder volume reduces, it becomes more difficult for the Cu concentration to remain constant.

Acknowledgment

This work was supported by the National Science Council through grants NSC98-2221-E-002-046-MY3.

References

[1] C.E. Ho, Y.L. Lin, C.R. Kao, Chem. Mater. 14 (2002) 949.
[2] C.E. Ho, R.Y. Tsai, Y.L. Lin, C.R. Kao, J. Electron. Mater. 31 (2002) 584.
[3] W.T. Chen, C.E. Ho, C.R. Kao, J. Mater. Res. 17 (2002) 263.
[4] L.C. Shiau, C.E. Ho, C.R. Kao, Solder. Surf. Mount. Technol. 14 (2002) 25.
[5] M.O. Alam, Y.C. Chan, K.N. Tu, Chem. Mater. 15 (2003) 4340.
[6] K.Y. Lee, M. Li, J. Electron. Mater. 32 (2003) 906.
[7] D.Q. Yu, C.M.L. Wu, D.P. He, N. Zhao, L. Wang, J.K.L. Lai, J. Mater. Res. 20 (2005) 2205.
[8] C.H. Lin, S.W. Chen, C.H. Wang, J. Electron. Mater. 31 (2002) 907.
[9] C.Y. Li, J.G. Duh, J. Mater. Res. 20 (2005) 3118.
[10] L. Sungovsky, P. Sungovsky, D.D. Perovic, J.W. Rutter, Mater. Sci. Technol. 22 (2006) 899.
[11] C. Schmetterer, H. Flandorfer, C.H. Luef, A. Kodentsov, H. Ipser, J. Electron. Mater. 38 (2009) 10.
[12] H. Yu, V. Vuorinen, J.K. Kivilahti, J. Electron. Mater. 36 (2007) 136.
[13] W.K. Choi, S.K. Kang, D.Y. Shih, J. Electron. Mater. 31 (2002) 1283.
[14] M.N. Islam, A. Sharif, Y.C. Chan, J. Electron. Mater. 34 (2005) 143.
[15] S.C. Yang, C.E. Ho, C.W. Chang, C.R. Kao, J. Appl. Phys. 101 (2007) 084911.
[16] S.C. Yang, Y.W. Wang, C.C. Chang, C.R. Kao, J. Electron. Mater. 37 (2008) 1591.
[17] M.H. Tsai, Y.W. Lin, C.R. Kao, J. Mater. Res. 24 (2009) 3407.
[18] C.E. Ho, Y.W. Lin, S.C. Yang, C.R. Kao, D.S. Jiang, J. Electron. Mater. 35 (2006) 1017.
[19] C.E. Ho, S.C. Yang, C.R. Kao, J. Mater. Sci. -Mater. Electron. 18 (2007) 155.
[20] C.K. Wong, J.H.L. Pang, J.W. Tew, B.K. Lok, H.J. Lu, F.L. Ng, Y.F. Sun, Microelectron. Reliabil. 48 (2008) 611.
[21] R. Darveaux, C. Reichman, C.J. Berry, W.S. Hsu, A. Syed, C.W. Kim, J.H. Ri, T.S. Kim, Proceedings of 2008 IEEE Electron. Comp. Tech. Conf. (ECTC) (2008) 113.
[22] C.W. Chang, S.C. Yang, C.T. Tu, C.R. Kao, J. Electron. Mater. 36 (2007) 1455.
[23] W.C. Luo, C.E. Ho, J.Y. Tsai, Y.L. Lin, C.R. Kao, Mater. Sci. Eng. A 396 (2005) 385.